Virus Research 290 (2020) 198188

Contents lists available at ScienceDirect

Virus Research

journal homepage: www.elsevier.com/locate/virusres

Selection and antigenic characterization of immune-escape mutants of H7N2 low pathogenic avian influenza virus using homologous polyclonal sera

Ioannis Sitaras [a], Erica Spackman [a,*], Mart C.M. de Jong [b], D. Joshua Parris [a]

[a] Exotic and Emerging Avian Viral Diseases Unit, Southeast Poultry Research Laboratory, United States National Poultry Research Center, United States Department of Agriculture, Agricultural Research Service, 934 College Station Road, Athens, GA, 30605, USA
[b] Quantitative Veterinary Epidemiology, Wageningen University and Research, Droevendaalsesteeg 1, 6708PB, Wageningen, The Netherlands

ARTICLE INFO

Keywords:
Low pathogenic avian influenza
Viral mutant selection
Polyclonal sera
Antigenic cartography
Virus evolution

ABSTRACT

Understanding the dynamics of the selection of influenza A immune escape variants by serum antibody is critical for designing effective vaccination programs for animals, especially poultry where large populations have a short generation time and may be vaccinated with high frequency. In this report, immune-escape mutants of A/turkey/New York/4450/1994 H7N2 low pathogenic avian influenza virus, were selected by serially passaging the virus in the presence of continuously increasing concentrations of homologous chicken polyclonal sera. Amino acid mutations were identified by sequencing the parental hemagglutinin (HA) gene and every 10 passages by both Sanger and deep sequencing, and the antigenic distance of the mutants to the parent strain was determined. Progressively, a total of five amino acid mutations were observed over the course of 30 passages. Based on their absence from the parental virus with deep sequencing, the mutations appear to have developed *de novo*. The antigenic distance between the selected mutants and the parent strain increased as the number of amino acid mutations accumulated and the concentration of antibodies had to be periodically increased to maintain the same reduction in virus titer during selection. This selection system demonstrates how H7 avian influenza viruses behave under selection with homologous sera, and provides a glimpse of their evolutionary dynamics, which can be applied to developing vaccination programs that maximize the effectiveness of a vaccine over time.

1. Introduction

Avian influenza viruses (AIV) are an important threat to animal health and food security. It is estimated that every year millions of birds die either as a direct result of avian influenza virus infections, or a result of biosecurity measures (such as culling of infected animals, pre-emptive culling, etc.) aiming to contain avian influenza outbreaks (Otte et al., 2008). Avian influenza viruses are classified by the OIE as either low pathogenic (LP) or highly pathogenic (HP) viruses based on their virulence in chickens. Of all the AIVs, those of the H5 and H7 subtypes are particularly important because they can mutate to the HP form (Bosch et al., 1981; Alexander, 2000; Suarez et al., 2004; Webster et al., 1986; Pappas et al., 2007), causing systemic infections and up to 100 % mortality in gallinaceous poultry. As such, LPAIVs of the H5 and H7 subtypes are particularly monitored and are notifiable to the world animal health organization (OIE). In much of the world, H5 and H7 LPAIVs are controlled by vaccination (Suarez et al., 2003). Most vaccines used in poultry worldwide (i.e. 95 %) are inactivated, adjuvanted whole virus vaccines (Swayne et al., 2011) which only induce serum polyclonal antibodies.

The surface proteins of influenza viruses are the targets of neutralizing antibodies. The hemagglutinin (HA), which outnumbers the neuraminidase by a ratio of 4:1 (Bouvier and Palese, 2008; Webster et al., 1992), experiences the most intense selection pressure from antibodies, and consequently is the most prone to mutations, which can alter its antigenicity sufficiently to avoid recognition by either natural infection-induced or vaccination-induced antibodies. Apart from reports of AIV mutants from the field, little is known on how immune pressure

Abbreviations: AIV, avian influenza virus; EID_{50}, 50% egg infectious dose; ECE, embryonating chicken egg; HA, hemagglutinin; HAU, hemagglutination units; HIU, hemagglutination inhibition units; HP, highly pathogenic; LP, low pathogenic; PBS, phosphate buffered saline; SPF, specific pathogen free.

* Corresponding author.
E-mail address: Erica.Spackman@usda.gov (E. Spackman).

https://doi.org/10.1016/j.virusres.2020.198188
Received 28 January 2020; Received in revised form 18 September 2020; Accepted 5 October 2020
Available online 10 October 2020

selects for immune escape mutants. Laboratory attempts to select for mutants of influenza viruses are frequently based on monoclonal antibodies, which are highly specific. Even when mixtures of monoclonal antibodies are used, this type of selection is not representative of what happens inside an animal, where the immune response against viruses is based on polyclonal antibodies, which have a much broader activity. A limited number of studies utilizing polyclonal serum have been published (Archetti and Horsfall, 1950; Cleveland et al., 1997), but have used static antibody levels. More importantly, polyclonal antibodies from the target host of vaccination, in this case chickens, are the most relevant to mimic selection pressure in the field.

In order to better understand the dynamics of how polyclonal antibodies select for escape mutants of LPAIVs, a well-characterized H7 lineage was utilized (Senne et al., 2003; Spackman et al., 2010; Spackman et al., 2003; Suarez et al., 1999). In addition to being well-characterized, this lineage was selected for its biological stability and safety because it has never become HP despite over a decade of circulation in live bird markets and occasional incursions into commercial poultry. An *in ovo* selection method first utilized with H5 HPAIV (Sitaras et al., 2014) was applied to A/turkey/New York/4450−4/1994 H7N2 LPAIV, by applying immune pressure in the form of continuously-increasing concentrations of homologous, chicken polyclonal sera. This method achieves selection through continuous rounds of refinement and changes were monitored by sequencing the HA gene and evaluating the antigenic distances of every fifth passage by antigenic cartography (Sitaras et al., 2014; Sitaras et al., 2019).

2. Materials and methods

2.1. Preparation of virus stock

A/turkey/New York/4450/1994 H7N2 LPAIV served as the parent strain (pass 0). The initial stock had been passaged in embryonating chicken eggs (ECEs) 3 times, which allowed for adaptation to ECE. A virus stock was prepared by passaging the virus once in specific pathogen free (SPF) 9 day-old ECEs using standard methods (Spackman and Stephens, 2016). Hemagglutination (HA) assays were performed to determine the HA titer from each egg. Allantoic fluids from all eggs that had HA titers within one $\log_2$ were pooled. The HA titer of the pooled virus stock was then determined and was found to be 128 (or $\log_2 7$) hemagglutination units (HAU). The virus was titrated in ECEs using standard methods (Spackman and Stephens, 2016) and was determined to be $10^{8.25}$ 50 % egg infectious doses (EID_{50}) per mL.

2.2. Polyclonal chicken serum

Homologous polyclonal sera were produced in 5 week-old SPF chickens. Procedures for all animal work were reviewed and approved by the US National Poultry Research Center Institutional Animal Care and Use Committee. Pass 0 virus was inactivated with 0.1 % β-propiolactone for 6−8 hours at room temperature and 4 °C overnight, after which the pH was adjusted to 7.0 using sodium bicarbonate. The HA titer of the inactivated virus was standardized to128 HAU per 0.025 mL. The inactivation was verified by failure to detect virus after two passages of 1% of the inactivated virus volume in ECEs by standard virus propagation methods (Spackman and Stephens, 2016).

Five SPF chickens were vaccinated intramuscularly with 0.5 mL of 128 HAU inactivated vaccine prepared with a mineral oil based adjuvant, Montanide™ ISA 70 V G, (SEPPIC Inc., Fairfield, NJ) at a 30 %:70 % inactivated virus:adjuvant ratio. Therefore, each 0.5 mL dose was comprised of 150 μL of inactivated virus and 350 μL of adjuvant. Three weeks post-vaccination, blood was collected, serum was separated and then inactivated at 56 °C for 50 min. Hemagglutination inhibition (HI) assays using the homologous inactivated virus as antigen (standardized to 4 HAU per 0.025 mL) were performed to evaluate the HI titer of the serum from each individual bird. All five sera were found to have HI titers within one $\log_2$ and were pooled. The HI titer of the pooled sera was confirmed by a HI assay and was found to be 512 (or $\log_2 9$) hemagglutination inhibition units (HIU) per 0.025 mL.

2.3. Determination of initial serum concentration for selection

Pass 0 virus was diluted in sterile phosphate buffered saline (PBS) to 16 HAU/0.025 mL, and the titer of the diluted virus was calculated to be $10^{6.5}EID_{50}$/mL. An optimum starting serum dilution for the selection experiments was defined as a dilution that results in a 1000-fold decrease in the EID_{50} titer. To determine the appropriate starting dilution for the serum, the parent strain (i.e. pass 0) was standardized to 16 HAU/0.025 mL and was incubated for 2 h at 37 °C with an equal volume of numerous concentrations of homologous sera. At the end of incubation the serum treated virus was titrated in 9 day-old ECEs to determine the reduction in titer. A 1:50 serum dilution (approximately 10.24 HIU) in sterile PBS produced an EID_{50} titer of $10^{3.6}$/mL and was thus considered as optimum for the start of the selection experiments.

2.4. Selection of mutants

Selection of immune escape mutants took place as originally described in (Sitaras et al., 2014). Briefly, for each round of selection, 16 HAU of virus from the previous passage (starting with pass 0) were incubated with an equal volume of homologous pooled sera, starting with ~10.24 HIU (1:50 dilution) determined as described above, for 2 h at 37 °C (Fig. 1).

As a control, during each round of selection 16 HAU of virus from the same selection round were incubated with an equal volume of the same dilution of non-immune sera (i.e. sera derived from SPF hens, free of antibody to AIV) as the dilution used for the selection with homologous immune sera. After the 2 h incubation, the control isolates were diluted 1000-fold in sterile PBS, in order to simulate the reduction in HA titer that has taken place in the antibody selected isolates.

After incubation, three 9- to 11-day-old ECEs were each inoculated with 200 μL of the antibody selected virus or the control virus. Inoculated ECEs were incubated at 37 °C for 48 h and were checked daily for embryo deaths. Dead embryos were removed from the incubator, time of death was recorded and placed at 4 °C pending harvesting of the allantoic fluid. At the end of the 48 h incubation period, allantoic fluid was harvested from all ECEs and HA assays were performed to determine the HA titer of the allantoic fluid from each individual egg. Allantoic fluid with titers within one $\log_2$ were pooled. The HA titer of the pooled allantoic fluids was then confirmed and diluted to 16 HAU/0.025 mL to be utilized in the next round of selection.

In total, 30 rounds of selection took place. The antibody concentration had to be periodically increased to maintain the same reduction in titer (Table 1). In the last rounds of selection, a 1:2 serum dilution was used, 25-fold higher than the starting serum dilution (Fig. 1).

2.5. Identification of mutations in the HA gene and variant analysis via deep sequencing

RNA from every fifth passage was isolated using the MagMAX™-96 AI/ND Viral RNA Isolation kit (ThermoFisher Scientific, Waltham, MA). For Sanger seqeuncing the HA gene was amplified using the OneStep RT-PCR kit (Qiagen, Germantown, MD), and primers specific for the HA of the parental strain that would allow amplification of the entire HA gene coding region. The product was run on a 1% agarose gel, the HA gene band was excised and the DNA was extracted using the QIAquick® Gel Extraction kit (Qiagen). The HA gene was sequenced with the BigDye dideoxy terminator kit (Life Technologies, Carlsbad, CA) using primers that spanned the entire coding region and overlapped, thus ensuring a minimum coverage of 3 reads. Sequencing results were analyzed using Lasergene (Version 15) (DNASTAR Madison, WI). The HA gene was translated into the HA protein and nucleotide substitutions resulting in

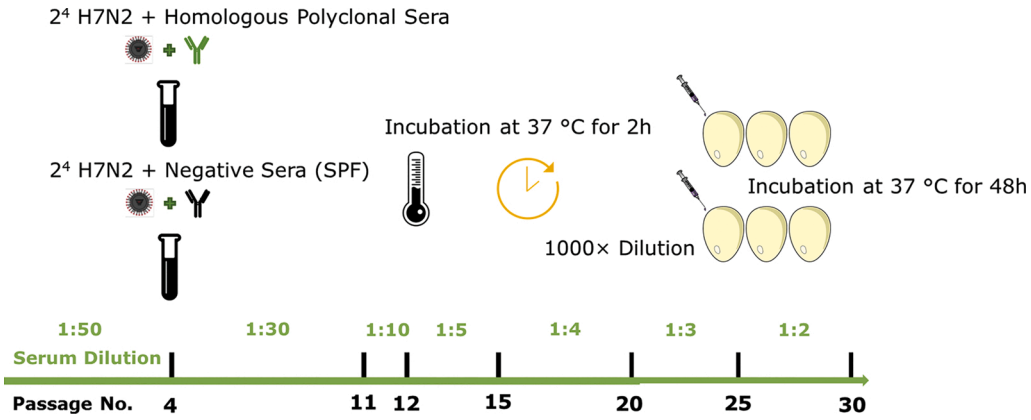

Fig. 1. Schematic representation of the protocol for selection of immune escape mutants. Increases in antibody concentration used throughout the passages are shown. Hemagglutination inhibition unit equivalents for serum concentrations are shown in Table 1.

Table 1
Concentrations of polyclonal chicken sera used during passaging. Control serum (influenza antibody-free serum) was used at the same dilution at the equivalent passages. HI titer of undiluted sera was 512 HIU.

Passage	Serum dilution	HIU[a]
1–3	1:50	10.24
4–10	1:30	17.07
11	1:10	51.2
12–14	1:5	102.4
15–19	1:4	128
20–24	1:3	170.67
25–30	1:2	256

a. HIU = hemagglutination inhibition unit.

amino acid changes were noted.

To determine if mutations in the HA gene were already present at low frequency in the quasispecies pool and arose progressively, serum treated material from passages 0, 10, 20, and 30 were selected for Next-Generation Sequencing (NGS). Briefly, isolated RNA was amplified via sequence independent, single primer amplification (SISPA), (Chrzastek et al., 2017). Sequencing libraries were prepared using the Nextera Flex kit (Illumina) and paired-end sequencing (2 × 250 bp) of the pooled libraries was performed on an Illumina MiSeq platform using the 300 cycle MiSeq Reagent Kit v 2 (Illumina, USA) according to manufacturer's instructions. Raw sequence reads were analyzed and assembled with MIRA v 3.4.1 (Chevreux et al., 2004) and read mapping from BWA-MEM (Li, 2013) was used to generate a consensus sequence for the HA gene within customized workflows on a Galaxy platform (Dimitrov et al., 2017). Variant analysis was performed in Geneious v 11.1.133 using alignment files and consensus sequences from Galaxy. Only variants with a p-value less than 0.05 occurring at a frequency greater than 1 % were considered.

2.6. Antigenic characterization of mutants

Sera against pass 0 and passages with amino acid changes (pass 10, 15, 20, 25, and 30) were raised in eight, 3 week-old chickens per passage. Each passage was inactivated using 0.02 % formalin. Inactivation was confirmed as described above. At this stage formalin was used for inactivation as opposed to β-propiolactone, to minimize potential chemical modifications to the HA that may affect virus binding (Bonnafous et al., 2014). Alterations of the HA protein could affect erythrocyte binding during the subsequent HI assays. The HA titers were standardized to 128 HAU/0.025 mL after inactivation. Vaccines were prepared with each passage and sera were produced in chickens as described above.

The HI dataset consisted of six antigens (virus passages 0, 10, 15, 20, 25 and 30) and eight homologous sera per each of the six antigens, for a total of 48 sera (each antigen was tested against 48 sera, out of which 8 sera were homologous to that antigen). All HI assays were performed in duplicate, and all antigens were cross-checked against all sera, resulting in 576 measurements in total. The procedure followed for distance calculations is the same as originally described in (Sitaras et al., 2014; Sitaras et al., 2019). All duplicate HI measurements were first averaged and then converted into $\log_2$ titers (e.g. 512 HIU converted into $\log_2 9$). This resulted in a 6 × 48 matrix. The difference between homologous and heterologous HI titers was calculated and standardized to be ≥0. The resulting 6 × 48 matrix shows the differences in HI titers between each one of the 6 passages against each of the 48 sera. The matrix was then standardized so that the average for each antigen against each serum would be 0 and the standard deviation would be 1. From this matrix, distances between strains were calculated using Mathematica® (Version 12, Wolfram Research Inc., Champaign, IL) by applying the distance formula:

$$distance_{i,j} = \sqrt{\sum_{k=1}^{48} \left(m_{i,k} - m_{j,k}\right)^2}$$

where m is a matrix element of matrix M.

The result was a 6 × 6 symmetrical master distance matrix, containing the distances between each possible pairwise comparison among the 6 strains. Note that such a matrix contains only 15 unique distances, i.e. the triangular matrix below the diagonal (Table 4). To construct an antigenic map showing the distances between different strains, any three sets of strains were compared by extracting the corresponding 3 × 3 sub-matrices from the master distance matrix, and solving the distance equation to obtain x and y coordinates. These strains are then plotted as triangles. By extracting sub-matrices the geometry between different strains is conserved since there is no distortion from reducing the dimensionality of the space in which the strains are plotted (Sitaras et al., 2014; Sitaras et al., 2019).

3. Results

3.1. Genetic characterization of mutants

The HA gene of every fifth passage of the selected and control viruses starting with the pass 0 was sequenced. In total, 7 nucleotide substitutions were selected by pass 30, resulting in 5 amino acid mutations (Table 2). Mutations were selected progressively and persisted in subsequent passages (Fig. 2). Only one nucleotide substitution was identified in pass 30 of the control isolates that were passaged identically with influenza antibody-free sera. It was the same A1062 G silent substitution observed from pass 15 onwards of the selected passages (H7 numbering

Table 2
Nucleotide and amino acid mutations selected in the presence of homologous polyclonal sera, compared to pass 0 (A/turkey/NY/4450-4/1994 H7N2 LPAI virus) by passage number.

Passage	Nucleotide substitutions	Amino acid mutations
5	–	-[a]
10	A1555G	S519G
15	T259C	F87L
	G641A	G214E
	A1062G	–
	A1555G	S519G
	T259C	F87L
20	G641A	G214E
	A1062G	–
	A1555G	S519G
	T259C	F87L
	G410A	G137E
	G641A	G214E
25	A1062G	–
	C1071T	–
	G1379A	R460H
	A1555G	S519G
	T259C	F87L
	G410A	G137E
	G641A	G214E
30	A1062G	–
	C1071T	–
	G1379A	R460H
	A1555G	S519G

a. A dash indicates a silent mutation.

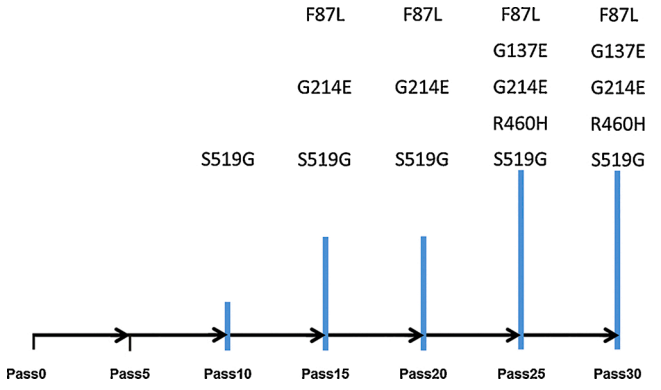

Fig. 2. Overview of amino acid mutations and the passage isolates in which they were selected. The height of the blue bars corresponds to the number of amino acid mutations.

is used throughout this report).

The first amino acid mutation was identified at pass 10 (S519 G). At that time, the antibody concentration had already been increased from 1:50 (10.24 HIU) to 1:30 (17.07 HIU) (Table 1). At pass 15 and pass 20 two additional amino acid mutations (F87 L and G214E) were selected. By passage 20, the antibody concentration had increased to 1:4 (128 HIU), 12.5× higher than the concentration used in the beginning of the selection process. At pass 25 the antibody concentration had increased to 1:2 (256 HIU, 25× higher than the starting serum concentration) and two more amino acid mutations (G137E and R460 H) were selected. All five amino acid changes were present at passage 30.

None of the nucleotide substitutions present at later passages were observed in the variant pool at passage 0 (Table 3). By passage 10, the A1555 G and G641A substitution sites showed a near equal distribution of variants and there was disagreement between NGS and Sanger sequencing as to which base to call in the consensus. Both of these substitutions would go to fixation by passage 20. The G410A substitution was detectable by deep sequencing in passage 20 at a frequency of 4.9 % (Table 3) and the minor variant would become a majority population by passage 25. Although NGS and Sanger were in agreement on the final consensus at passage 30, four of the seven cumulative substitutions could not be detected with deep sequencing at the given sampling frequency. Additional variable sites including G1654A were identified via deep sequencing but never became fixed in later passages (Table 3).

3.2. Antigenic characterization of mutants

The antigenic differences among the selected passages were evaluated by means of a series of HI assays in which all strains were cross-checked against all sera. All measurements were performed in duplicate; almost all had the same HI titer and in only a few cases a difference of one $\log_2$ was observed. The duplicate measurements taken proved to be extremely consistent, with almost all showing the same HI titer and only a few cases where a difference of one $\log_2$ was observed. The difference between the antibody titers mounted within each group of 8 animals vaccinated with the same vaccine was mostly $\log_2 2$-$\log_2 3$ with some cases being as high as $\log_2 4$ or as low as one $\log_2$.

From the results of the HI assays, antigenic distances were calculated and a master distance matrix was created (Table 4). Antigenic maps were constructed from the master distance matrix by extracting submatrices corresponding to the passages that are to be compared. Because no amino acid mutations were found in pass 5, serum against this strain was not raised and it was excluded from antigenic characterization.

The distance of each passage from the pass 0 consistently increased with passage number and accumulation of amino acid mutations (Fig. 3). The largest antigenic distance observed was between pass 0 and pass 30 ($\log_2 3.85$ or 14.42 HIU).

4. Discussion

The results show that the method used was successful in selecting for mutants able to escape antibody pressure from homologous polyclonal sera. The fact that continuously higher concentrations of antibody was needed to reduce virus titer and to select for additional amino acid mutations, implies that these mutations were selected as a direct result of antibody pressure.

Some work with monoclonal antibodies has been reported to characterize the antigenic sites of the H7 HA (Schmeisser et al., 2015; Yao et al., 2019). Here the location of the mutations was inferred from previously identified dominant epitopes on the HA of H3 and H5 subtypes (Duvvuri et al., 2009; Criado et al., 2019; Wiley et al., 1981), and through an alignment between the sequence of our H7 influenza viruses and the H5N1 A/goose/Guangdong/1/96 reference strain. Two of the amino acid mutations we selected appear to be located in previously defined dominant epitopes in the HA (F87 L and G214E located in epitopes E and D respectively) (Fig. 4) (Criado et al., 2019). The remaining three amino acid mutations (G137E, R460H, S519 G) were found to be either adjacent to, or in other areas of previously defined antigenic significance (Duvvuri et al., 2009; Criado et al., 2019; Wiley et al., 1981). Mutation G137E is wedged between the amino acids forming antigenic epitope A, and mutations R460H and S519 G appear to be in the membrane-proximal part of the HA stalk domain. Position 460 in particular (or 468 in H1 numbering), is identified as the only positive selection site in the HA stalk (Duvvuri et al., 2009; Kirkpatrick et al., 2018). In addition, the mutation to glycine may confer flexibility to the ectodomain, thus have an indirect effect in the way antibodies recognize and bind to it (Benton et al., 2018). Antibodies to the HA stalk domain have been shown to provide broadly reactive immunity (Wang et al., 2017; Zhang et al., 2017) and are the focus of universal vaccines. Although it was originally believed that the HA stalk domain is not susceptible to immune pressure and does not evolve, recent research has shown that the stalk domain is evolving, albeit at a much slower rate than the HA head (Kirkpatrick et al., 2018) and that immune pressure on

Table 3
Variable sites in the HA gene identified from deep sequencing. Only variants occurring at a frequency greater than 2% are shown here. Sites in bold font indicate mutations that became fixed in the consensus sequence for later passages.

Passage	Position	Change	Amino Acid Change	Coverage	Variant Frequency	Variant P-Value (approximate)
0	1654	G -> A	G -> R	240	8.30 %	7.10E-48
	1050	G -> A		1035	24.80%	0
	876	T -> C		734	27.90%	0
	674	T -> G	I -> S	696	25.90%	0
	584	G -> T	G -> V	745	27.00%	0
	427	A -> G	T -> A	736	32.20%	0
	336	T -> C		803	28.00%	0
10	1654	G -> A	G -> R	853	7.70 %	5.40E-152
	1555	G -> A	G -> S	2902	36.90%	0
	641	A -> G	E -> G	2345	39.50 %	0
	593	G -> T	S -> I	2251	3.40%	1.00E-146
	356	T -> C	I -> T	2234	2.60%	1.70E-103
	130	G -> A	V -> I	1506	3.50 %	7.80E-104
20	1671	T -> C		1419	38.50 %	0
	1654	G -> A	G -> R	2020	4.40%	5.90E-182
	410	G -> A	G -> E	7075	4.90%	0
	170	A -> G	K -> R	6251	2.40%	1.30E-275
30	1654	G -> A	G -> R	101	3.00%	3.30E-07
	1464	G -> A	M -> I	318	44.00%	0
	1135	A -> G	S -> G	285	2.10%	1.10E-11
	266	A -> T	E -> V	238	2.10%	5.90E-10

Table 4
Antigenic distance matrix used for the construction of antigenic maps. Distances are $\log_2$ values (i.e. 3.85 is $\log_2$3.85, or 14.42 HIU). The matrix is symmetrical.

Passage	Passage					
	0	10	15	20	25	30
0	0					
10	1.19	0				
15	2.17	1.18	0			
20	2.24	1.18	0.37	0		
25	3.10	2.15	1.59	1.37	0	
30	3.85	3.16	2.36	2.34	1.51	0

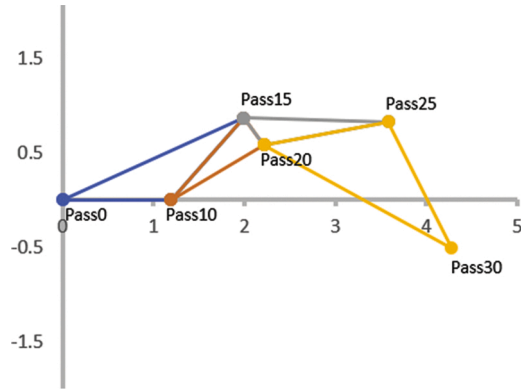

Fig. 3. Antigenic map showing the distances between and among passage isolates. All distances between passage isolates connected with a line are the same distances as calculated and reported in the master distance matrix. To show distances between sets of passage isolates other than the ones shown in this map (i.e. pass 0, pass 25 and pass 30), the relevant sub-matrices need to be extracted. Distances are shown in $\log_2$ values corresponding to hemagglutination inhibition units (i.e. $\log_2 4 = 16$ HIU) on both the X and Y axis.

the stalk domain can indeed lead to the selection of mutants that are able to escape immunity from broadly neutralizing antibodies, such as the ones elicited by universal vaccines (Wu et al., 2020; Park et al., 2020). Whether our selected mutations located in the HA stalk would render a universal vaccine ineffective is a matter of speculation since we did not carry out this particular research. However, it would be safe to assume that if any mutations in the HA stalk would alter the antigenic distance between the parent strain and the mutant sufficiently, or would result in somehow altering the conformation of the HA stalk, then we would expect that the efficiency of the broadly neutralizing antibodies of universal vaccines would be compromised also.

Even if some of the mutations selected were not located in known antigenic epitopes, the fact that the polyclonal serum selected these amino acid mutations and the antigenic distance from pass 0 increased with additional mutations, suggests that they are antigenically-important. The absence of amino acid mutations in the control passages treated with influenza antibody-free serum, and the fact that the mutations appear to have become fixed in the selected passages provides further support that these sites are important for neutralizing antibody binding.

Because most of the nucleotide substitutions translated into amino acid mutations, we can deduce that our selection method is very "economical", in that silent mutations are few. Indeed, we can assume that our selection method is Darwinian, only mutations necessary for virus survival under continuously increased antibody pressure are selected and no "energy" is wasted in silent mutations. This is also supported by the fact that no amino acid mutations were found in the control isolates, as there was no survival reason for the virus to select for mutants in those isolates. Additionally, deep sequencing showed these mutations were not present in the starting population and arose *de novo* as a result of selection pressure. Only 3 of the 7 substitutions observed at passage 30 could be detected in variant analysis of the earlier passages selected for deep sequencing suggesting mutations beneficial to virus survival went to fixation rapidly once present in the population. Additional variants not in the final consensus arose at various stages of the passages but never went to fixation further demonstrating only beneficial substitutions persisted.

Antigenic characterization shows that the distance between the passages increased with the accumulation of amino acid mutations. In other words, successive passages drifted away not only from the parent strain (pass 0), but from each other. The maximum distance observed was between pass 0 and pass 30 and was calculated to be $\log_2$3.85 (14.45 HIU). Importantly, the fact that we raised sera against each strain in more than one animal, eliminates the effect of inter-individual variation in vaccination-induced immune response, and makes our distance calculations (and consequently our antigenic maps) more accurate, as discussed in (Sitaras et al., 2019), thus maintaining real distances between each set of compared strains, and conserving the geometry of

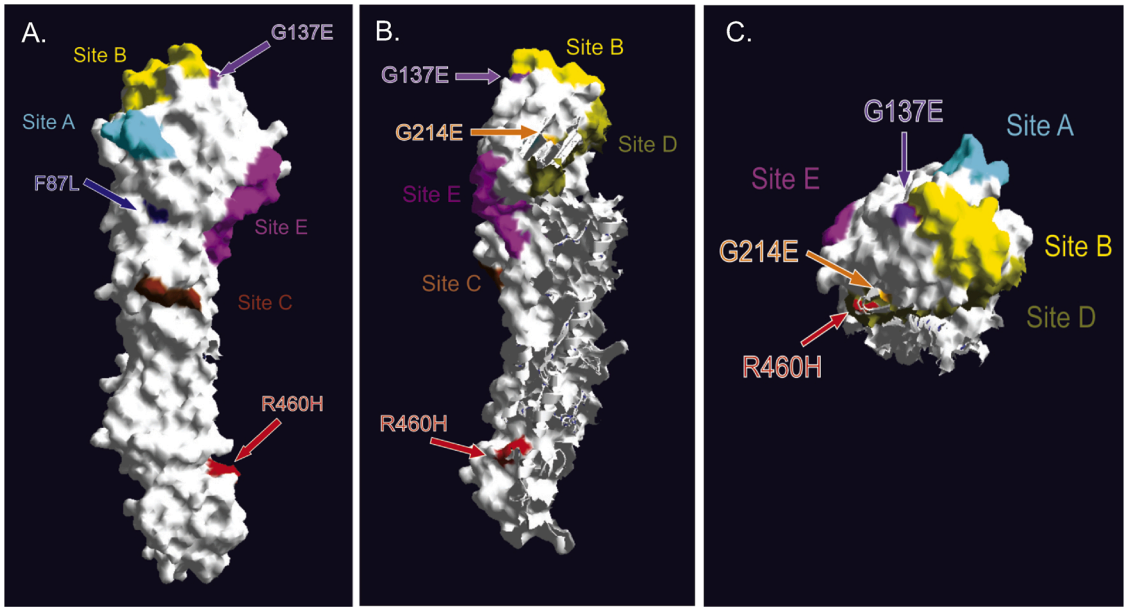

Fig. 4. Cartoon of the H7 HA monomer deduced protein structure (Van der Waals surface) of the H7 HA of A/turkey/NY/4450-4/1994 with the correlating H3 dominant antigenic sites (Criado et al., 2019) and amino acid changes observed here shown. A) side view; B) alternate side-view; and C) top view. The model was built with SWISS-MODEL using A/Victoria/361/2011 H3N2 as a template and the cartoon was make with DeepView/Swiss-pdb viewer v4.1.0 (Bienert et al., 2017; Waterhouse et al., 2018; Guex et al., 2009).

shape-space.

When the amino acid sequences are the same, as in the case of pass 15 and pass 20, the antigenic distance between the two strains is very small, as would be expected, because the strains are closely related. These small differences have to do with the way mutants are selected. Influenza virus populations contain numerous subpopulations (quasispecies) carrying different mutations, with one quasispecies being substantially more dominant than the rest. This selection method neutralizes the dominant quasispecies and progressively increases the abundance of another population which carries mutations that allow it to survive against the applied antibody pressure. Every passage is a further round of refinement. As a consequence, even when two passages may have the exact same amino acid sequences in the dominant quasispecies as determined with Sanger sequencing, the later passage represents a more refined population, therefore a small antigenic distance may be observed. Also important for understanding the dynamics is that because the variants appear to arise *de novo*, it is possible that variants may be different among the 3 eggs. Because the material is pooled after the virus has replicated, the variants are mixed for the subsequent round of selection and the most fit variants will likely be selected from the pooled population

A comparison between this work and a similar study with goose/Guangdong/1996 lineage H5N1 HPAIV where the selection protocol was reported for the first time (Sitaras et al., 2014), draws some interesting conclusions. It is evident that the selection system works equally well with both HPAI and LPAI influenza viruses of either H5 and H7 subtypes. Indeed, the results of the current research are very similar to results obtained when selecting for immune escape mutants of HPAI H5N1 (Sitaras et al., 2014) and H7N7 viruses (unpublished data). In particular, in both this report and in (Sitaras et al., 2014) the immune pressure needs to be increased throughout the selection process, amino acid mutations appear to be selected faster when the immune pressure is increased, antigenic distance increases with the accumulation of amino acid mutations, and no amino acid mutations are selected in the control isolates. It is noteworthy that the distance between pass 0 and pass 30 (14.45 HIU) found in this report is larger than the distance between the parent strain HPAI H5N1 (A/turkey/Turkey/1/2005) and the latest passage isolate, Pass42 (4.5 HIU) found in (Sitaras et al., 2014). This can be due to the fact that in (Sitaras et al., 2014), a more conservative approach to selection was taken, in that the serum pressure started to be continuously increased only after the 20th passage.

Similarly, a comparison between this work and the situation in the field, particularly in the case of H7N3 viruses in Italy and H7N9 viruses in China where vaccination has been used as a control measure, allows us to draw some interesting conclusions. In Italy, it has been demonstrated that although some positive selection pressure appears to be caused by vaccination, the viruses isolated from vaccinated animals appeared to be more antigenically-similar than the viruses isolated from unvaccinated animals. In addition, one of the mutations identified in the Italian isolates after vaccination (G144E, H3 numbering) appears to be the same as the G137E (H7 numbering) mutation we report in our isolates (Beato et al., 2014). In the case of H7N9 viruses in China, there are similar concerns that antigenic variants may emerge in unvaccinated birds, and although some mutants were identified after vaccination was applied, no antigenic analysis has been performed to-date to allow us to know whether these mutants are sufficiently antigenically-different to evade vaccination-induced immunity (Zeng et al., 2018; Yu et al., 2019). One of the H7N9 mutants identified in China carried an amino acid mutation at position 221 (H3 numbering), which is the same as position 214 (H7 numbering), where we selected for mutation G214E (Jiang et al., 2019).

The dynamics of the selection process are important for developing effective vaccination programs for poultry in the field. Specifically, the results presented here demonstrate and confirm that with time, higher titers of antibody from a vaccine are needed to neutralize the virus as it continues to circulate. Higher doses and more frequent administration of vaccine would be necessary to maintain efficacy in the field until a replacement vaccine can be produced. This is especially true when the reproductive ratio of the challenge (field) virus in vaccinated animals is above 1, since if it is below 1, immune-escape mutants should not be selected. Practically, increasing the vaccine dose and frequency in the field can be difficult because this approach is resource intensive, especially for long term vaccination of long-lived birds (i.e. layers or breeders). Ring vaccination of targeted populations may be more able to maintain high levels of immunity. The goal of vaccination, for example minimizing production losses versus halting spread, will also factor into

the cost-benefit of this approach. Requiring minimum potency from manufacturers will help assure adequate doses can be applied.

It is also possible that if the antibody concentration were to remain the same, mutations may not continue to be selected, or the process may be much slower. Practically, this suggests that vaccines which are highly immunogenic and/or highly potent, but which are under the threshold to completely halt transmission in a population, may select escape mutants faster. It is also unknown whether the changes which can occur are restricted or whether there are alternative pathways for escape. An additional limitation is that we did not evaluate the role of the NA. Notably, AIV vaccines for poultry are often selected because they express a different NA subtype than the field virus to aid in differentiating infected from vaccinated animals (Suarez, 2012), so the practical implications are not clear with current vaccine practices. Selection of subpopulations and *de novo* mutations, are both likely to occur in the field.

5. Conclusions

Antibody escape mutants of an H7N2 LPAIV have been selected by using homologous chicken polyclonal sera. Although we cannot completely exclude the possibility of any mutants that can escape in the original virus population, they were not observed in the deep sequencing data, therefore the escape mutants appear to have arisen *de novo*. After 30 rounds of selection, five amino acid changes were observed in the HA protein. Periodic increases in antibody concentration was necessary during the selection process to maintain consistent levels of reductions in virus titers as more mutations accumulated. Antigenic characterization of the mutants has shown that the antigenic distance increased with the number of mutations and passage number. These dynamics suggest that designing vaccination programs with sufficiently high efficacy to halt transmission, rather than to just reduce production losses, could extend the life of a vaccine seed strain.

Ethics statement

All protocols and procedures involving animals were reviewed and approved by the USNRC animal care and use committee.

CRediT authorship contribution statement

Ioannis Sitaras: Conceptualization, Methodology, Software, Validation, Formal analysis, Investigation, Data curation, Writing - original draft, Visualization. **Erica Spackman:** Conceptualization, Methodology, Formal analysis, Resources, Writing - original draft, Visualization, Supervision, Project administration. **Mart C.M. de Jong:** Methodology, Software, Formal analysis, Writing - review & editing. **D. Joshua Parris:** Methodology, Validation, Formal analysis, Investigation, Data curation, Writing - review & editing, Visualization.

Acknowledgements

The authors gratefully acknowledge: Christopher Stephens, Scott Lee, Jesse Gallagher, Dawn Williams-Coplin, Keith Crawford, Gerald Damron, and Roger Brock for technical assistance with this work. This research was supported by US Department of Agriculture, ARS CRIS Project6040-32000-066-00D and USDA-APHIS Agreement#60-6040-6-005. Mention of trade names or commercial products in this manuscript is solely for the purpose of providing specific information and does not imply recommendation or endorsement by the U.S. Department of Agriculture. USDA is an equal opportunity provider and employer.

References

Otte, J., Hinrichs, J., Rushton, J., Roland-Holst, D., Zilberman, D., 2008. Impacts of avian influenza virus on animal production in developing countries. CAB Rev. Perspect. Agri. Vet. Sci. Nutr. Nat. Res. 3, 1–18.
Bosch, F.X., Garten, W., Klenk, H.D., Rott, R., 1981. Proteolytic cleavage of influenza virus hemagglutinins: primary structure of the connecting peptide between HA1 and HA2 determines proteolytic cleavability and pathogenicity of Avian influenza viruses. Virology 113, 725–735.
Alexander, D.J., 2000. A review of avian influenza in different bird species. Vet. Microbiol. 74, 3–13.
Suarez, D.L., Senne, D.A., Banks, J., Brown, I.H., Essen, S.C., Lee, C.W., et al., 2004. Recombination resulting in virulence shift in avian influenza outbreak, Chile. Emerging Infect. Dis. 10, 693–699.
Webster, R.G., Kawaoka, Y., Bean Jr., W.J., 1986. Molecular changes in A/Chicken/Pennsylvania/83 (H5N2) influenza virus associated with acquisition of virulence. Virology 149, 165–173.
Pappas, C., Matsuoka, Y., Swayne, D.E., Donis, R.O., 2007. Development and evaluation of an Influenza virus subtype H7N2 vaccine candidate for pandemic preparedness. Clin. Vaccine Immunol. 14, 1425–1432.
Suarez, D.L., Spackman, E., Senne, D.A., 2003. Update on molecular epidemiology of H1, H5, and H7 influenza virus infections in poultry in North America. Avian Dis. 47, 888–897.
Swayne, D.E., Pavade, G., Hamilton, K., Vallat, B., Miyagishima, K., 2011. Assessment of national strategies for control of high-pathogenicity avian influenza and low-pathogenicity notifiable avian influenza in poultry, with emphasis on vaccines and vaccination. Revue Scientifique et Tech. 30, 839–870.
Bouvier, N.M., Palese, P., 2008. The biology of influenza viruses. Vaccine 26 (Suppl 4), D49–53.
Webster, R.G., Bean, W.J., Gorman, O.T., Chambers, T.M., Kawaoka, Y., 1992. Evolution and ecology of influenza A viruses. Microbiol. Rev. 56, 152–179.
Archetti, I., Horsfall Jr., F.L., 1950. Persistent antigenic variation of influenza A viruses after incomplete neutralization in ovo with heterologous immune serum. J. Exp. Med. 92, 441–462.
Cleveland, S.M., Taylor, H.P., Dimmock, N.J., 1997. Selection of neutralizing antibody escape mutants with type A influenza virus HA-specific polyclonal antisera: possible significance for antigenic drift. Epidemiol. Infect. 118, 149–154.
Senne, D.A., Suarez, D.L., Pedersen, J.C., Panigrahy, B., 2003. Molecular and biological characteristics of H5 and H7 avian influenza viruses in live-bird markets of the Northeastern United States, 1994-2001. Avian Dis. 47, 898–904.
Spackman, E., Gelb Jr., J., Preskenis, L.A., Ladman, B.S., Pope, C.R., Pantin-Jackwood, M.J., et al., 2010. The pathogenesis of low pathogenicity H7 avian influenza viruses in chickens, ducks and turkeys. Virol. J. 7, 331.
Spackman, E., Senne, D.A., Davison, S., Suarez, D.L., 2003. Sequence analysis of recent H7 avian influenza viruses associated with three different outbreaks in commercial poultry in the United States. J. Virol. 77, 13399–13402.
Suarez, D.L., Garcia, M., Latimer, J., Senne, D., Perdue, M., 1999. Phylogenetic analysis of H7 avian influenza viruses isolated from the live bird markets of the Northeast United States. J. Virol. 73, 3567–3573.
Sitaras, I., Kalthoff, D., Beer, M., Peeters, B., de Jong, M.C., 2014. Immune escape mutants of highly pathogenic avian influenza H5N1 selected using polyclonal sera: identification of key amino acids in the HA protein. PLoS One 9, e84628.
Sitaras, I., Duijzer, M., Peeters, B., de Jong, M.C., 2019. Influence of inter-animal variability of HI Titres on antigenic cartography in the study of avian influenza viruses: towards making a better map. Heliyon. Submitted Manuscript.
Spackman, E., Stephens, C., 2016. Virus isolation and propagation in embryonated eggs. In: Williams, S.M. (Ed.), A Laboratory Manual for the Isolation, Identification and Characterization of Avian Pathogens, 6th ed. American Association of Avian Pathologists, pp. 361–368.
Chrzastek, K., Lee, D.H., Smith, D., Sharma, P., Suarez, D.L., Pantin-Jackwood, M., et al., 2017. Use of Sequence-Independent, Single-Primer-Amplification (SISPA) for rapid detection, identification, and characterization of avian RNA viruses. Virology 509, 159–166.
Chevreux, B., Pfisterer, T., Drescher, B., Driesel, A.J., Muller, W.E., Wetter, T., et al., 2004. Using the miraEST assembler for reliable and automated mRNA transcript assembly and SNP detection in sequenced ESTs. Genome Res. 14, 1147–1159.
Li, H., 2013. Aligning sequence reads, clone sequences and assembly contigs with BWA-MEM. Arxivorg.
Dimitrov, K.M., Sharma, P., Volkening, J.D., Goraichuk, I.V., Wajid, A., Rehmani, S.F., et al., 2017. A robust and cost-effective approach to sequence and analyze complete genomes of small RNA viruses. Virol. J. 14, 72.
Bonnafous, P., Nicolai, M.C., Taveau, J.C., Chevalier, M., Barriere, F., Medina, J., et al., 2014. Treatment of influenza virus with beta-propiolactone alters viral membrane fusion. Biochim. Biophys. Acta 1838, 355–363.
Schmeisser, F., Vasudevan, A., Verma, S., Wang, W., Alvarado, E., Weiss, C., et al., 2015. Antibodies to antigenic site A of influenza H7 hemagglutinin provide protection against H7N9 challenge. PLoS One 10, e0117108.
Yao, L., Chen, Y., Wang, X., Bi, Z., Xiao, Q., Lei, J., et al., 2019. Identification of antigenic epitopes in the haemagglutinin protein of H7 avian influenza virus. Avian Pathol. 1–12.
Duvvuri, V.R., Duvvuri, B., Cuff, W.R., Wu, G.E., Wu, J., 2009. Role of positive selection pressure on the evolution of H5N1 hemagglutinin. Genomics Proteomics Bioinf. 7, 47–56. Beijing Genomics Institute.
Criado, M.F., Bertran, K., Lee, D.H., Killmaster, L., Stephens, C.B., Spackman, E., et al., 2019. Efficacy of novel recombinant fowlpox vaccine against recent Mexican H7N3 highly pathogenic avian influenza virus. Vaccine 37, 2232–2243.

Wiley, D.C., Wilson, I.A., Skehel, J.J., 1981. Structural identification of the antibody-binding sites of Hong Kong influenza haemagglutinin and their involvement in antigenic variation. Nature 289, 373–378.
Kirkpatrick, E., Qiu, X., Wilson, P.C., Bahl, J., Krammer, F., 2018. The influenza virus hemagglutinin head evolves faster than the stalk domain. Sci. Rep. 8, 10432.
Benton, D.J., Nans, A., Calder, L.J., Turner, J., Neu, U., Lin, Y.P., et al., 2018. Influenza hemagglutinin membrane anchor. Proc. Natl. Acad. Sci. U.S.A. 115, 10112–10117.
Wang, Y., Wu, J., Xue, C., Wu, Z., Lin, Y., Wei, Y., et al., 2017. A recombinant H7N9 influenza vaccine with the H7 hemagglutinin transmembrane domain replaced by the H3 domain induces increased cross-reactive antibodies and improved interclade protection in mice. Antiviral Res. 143, 97–105.
Zhang, Y., Wei, Y., Liu, K., Huang, M., Li, R., Wang, Y., et al., 2017. Recombinant influenza H9N2 virus with a substitution of H3 hemagglutinin transmembrane domain showed enhanced immunogenicity in mice and chicken. Sci. Rep. 7, 17923.
Wu, N.C., Thompson, A.J., Lee, J.M., Su, W., Arlian, B.M., Xie, J., et al., 2020. Different genetic barriers for resistance to HA stem antibodies in influenza H3 and H1 viruses. Science 368, 1335–1340.
Park, J.K., Xiao, Y., Ramuta, M.D., Rosas, L.A., Fong, S., Matthews, A.M., et al., 2020. Pre-existing immunity to influenza virus hemagglutinin stalk might drive selection for antibody-escape mutant viruses in a human challenge model. Nat. Med. 26, 1240–1246.
Beato, M.S., Xu, Y., Long, L.P., Capua, I., Wan, X.F., 2014. Antigenic and genetic evolution of low-pathogenicity avian influenza viruses of subtype H7N3 following heterologous vaccination. Clin. Vaccine Immunol. 21, 603–612.
Zeng, X., Tian, G., Shi, J., Deng, G., Li, C., Chen, H., 2018. Vaccination of poultry successfully eliminated human infection with H7N9 virus in China. Sci. China Life Sci. 61, 1465–1473.
Yu, D., Xiang, G., Zhu, W., Lei, X., Li, B., Meng, Y., et al., 2019. The re-emergence of highly pathogenic avian influenza H7N9 viruses in humans in mainland China. Euro Surveill. 2019, 24.
Jiang, W., Hou, G., Li, J., Peng, C., Wang, S., Liu, S., et al., 2019. Antigenic variant of highly pathogenic avian influenza a(H7N9) virus, China. Emerging Infect. Dis. 2020, 26.
Suarez, D.L., 2012. DIVA vaccination strategies for avian influenza virus. Avian Dis. 56, 836–844.
Bienert, S., Waterhouse, A., de Beer, T.A., Tauriello, G., Studer, G., Bordoli, L., et al., 2017. The SWISS-MODEL repository-new features and functionality. Nucleic Acids Res. 45. D313-D9.
Waterhouse, A., Bertoni, M., Bienert, S., Studer, G., Tauriello, G., Gumienny, R., et al., 2018. SWISS-MODEL: homology modelling of protein structures and complexes. Nucleic Acids Res. 46, W296–W303.
Guex, N., Peitsch, M.C., Schwede, T., 2009. Automated comparative protein structure modeling with SWISS-MODEL and Swiss-PdbViewer: a historical perspective. Electrophoresis 30 (Suppl 1), S162–73.